A Quantum Model of Linear Optical Devices for Quantum Computing

Yuan Jiang and Rebecca Jiang[a)]

(Dated: 16 November 2020)

Extending an existing quantum optic model for beamsplitters, a comprehensive model is developed from the first principles of quantum physics to describe photons traversing linear optical devices of arbitrary number of ports and even a circuit of devices, which are essential components of photonic quantum computing gates and circuits. The model derives the quantum operators and states of the photons at the egress ports of a device, gate or circuit from those at the ingress ports. As an application and validation, it is used to model the experiment that discovered the Hong-Ou-Mandel (HOM) effect. The experiment is not only a landmark in the research of quantum optics but also important to photonic quantum computing design.

I. INTRODUCTION

Quantum computing has generated great attention in research. The proposal that a complete set of universal quantum computing gates – Hadamard, phase shift and control-not (C-NOT) gates – can be made mainly from linear optical devices including phase-shift plates, mirrors and beamsplitters[1] is particularly exciting and has been named after the authors Knill et al as the KLM protocol. With advanced integrated photonic technologies, hundreds of such devices concatenated or otherwise connected can be made into not only gates but also circuits[2]. The ingress side of a gate or circuit not only has photons carrying information of qubits entering its input ports, but may also have ancilla photons carrying no information entering ancilla ports[13]. Similarly on the egress side, it may have information carrying photons exiting its output ports and ancilla photons measured or discarded at the rest of the egress ports. To study and design such increasingly complicated gates and circuits operating in the quantum regime of one or a few photons, we need a sophisticated quantum optic model. Even while some of the research attention has shifted from the KLM protocol to cluster state quantum computing scheme, linear optical devices are still widely used and their quantum model remain important[4].

While quantum models for single or dual port devices exist, none exists for multiple port or circuits of devices. Mirrors and phase-shift plates are single (one ingress and one egress) port devices, and their quantum models are trivial. Beamsplitters, which are dual-port devices used in building Hadamard and C-NOT gates, have gone through extensive study and have many quantum models. Most models treat a beamsplitter as a black box, assume it destroys the photons entering the ingress ports and recreates them before they exit the egress. Such a black-box model needs to impose restrictions such as energy conservation to derive how the egressing photons relate to ingressing ones[1,5]. One even needs to impose SU(2) subgroup restriction[6] and concludes that beamsplitters cause fourth-order interference in the quantum regime[7].

a)Electronic mail: yjj@xanatech.com

We find only one model, by Fearn and Loudon,[8] that is derived from the first principles of quantum physics. However, it is not as easy to derive and understand as the blackbox models, and thus is mostly not used.

The shortcomings of the black-box models become obvious in the modeling of gates and circuits for quantum computing. They not only cannot be adopted to model multiple port devices or circuits of devices, but also could be wrongly used to infer what goes on inside the black boxes – it has been inferred that one photon impinging on a beamsplitter port causes 90-degree phase shift of another impinging on the second port[9,10] and results in the so-called quantum interference. Not the least, such incorrect inference has even been used in the design of quantum computing gates[11].

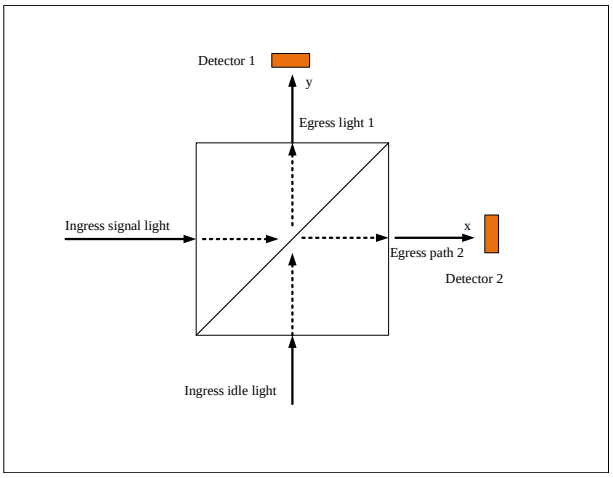

FIG. 1. Schematic of HOM experiment in which signal and idler photons from parametric down converter enter a beam splitter's ingress ports and exit its egress ports 1 and 2.

The inference of quantum interference has its origin in the Hong-Ou-Mandel (HOM) experiment[9]. The experiment shows that when two indistinguishable pulsed photons (signal and idler photons from optical down conversion) go through a beamsplitter as shown in the simplified scheme in Fig.1, the probability of detecting coincidentally at both detectors placed respectively in the two egress paths dips to zero when the optical paths from the source of the photons to the two detectors are equal.

Such a coincidental detection dip is called the HOM effect, named after the authors Hong et al, and has been demonstrated repeatedly. Followup experiments demonstrating the same or similar effect have used various setups including replacing the beamsplitter with a fiber four-way mixer[12] or similar passive optical devices[13], or replacing the photon sources with two-trapped atoms[14] or a single quantum dot[15]. The HOM experiment is a landmark in demonstrating the quantum nature of photons and is influential to quantum computing in the following ways:

- the photon generation, detection and manipulation techniques used in it are widely used in today's research on quantum computing[16],
- the blackbox model used to model the experiment is also used in quantum computing research,
- the inference of quantum interference has been used in the design of quantum computing gates[11].

In this article, we extend the Fearn and Loudon model to a quantum model for generic linear optical devices or circuits of devices in Section III. Before that, we introduce the classical mode model in Section II. In both sections, we exemplify and validate the models by applying them to the HOM experiment.

II. THE CLASSICAL WAVE MODEL

A. Electric field and modes

We first start with the classical wave model, which 1) establishes the mode model to be used in the quantum model and 2) offers insight to the HOM effect. In the simplest case, the signal light in Fig.1 is a traveling plain wave propagating in the x-axis direction towards the beamsplitter, and its electric field wave function is

$$E_s(x, y, z, \tau) = E_0 e^{i(k_s x - \omega_s \tau)} \tag{1}$$

where k_s and ω_s are the signal light's wavevector and angular frequency respectively, and $k_s = c\omega_s$. We use τ instead of t for time to avoid confusion with transmitance t, which will be used below. The electric field is expressed as the product of amplitude E_0 and a mode function, which satisfies Maxwell equations and the boundary conditions. We can generalize the wave function to cover experiments conducted using optical fibers by including the lateral mode functions $u(y, z)$ and $u(z, y)$ – assuming fibers are placed in the x and y-axis directions. We can write the above electric field as

$$E_s(x, y, z, \tau) = E_0 u(y, z) e^{i(k_s x - \omega_s \tau)} \tag{2}$$

Without losing generality, we ignore details such as polarization (i.e. by assuming polarization in the z direction). We also assume each of the fibers supports only one lateral mode u and the longitudinal wavevector $k_s = c\omega_s$ is true. Obviously, in the extreme case of $u(y, z) = 1$, the expression is no different from a plane wave. So, we will use equation 2 in the following discussion. Of course, similarly to the idler light, we can write the electric field $E_i(x, y, z, \tau)$ traveling along the y-axis toward the beamsplitter.

As shown in Fig. 1, the beamsplitter splits the ingress signal and idler lights each into two paths on the egress side. Two detectors, 1 and 2, are placed on the two egress paths. We shall assume that the beamsplitter being placed at the coordinate origin at first before being displaced to a d distance from the origin and that the detectors are placed at distance D from the coordinate origin. d is a variable in the experiment, and different values of d lead to different observation in the detectors. We make similar assumptions of the optical fiber versions of beamsplitters so that we are not bogged down by the physical details. In the classical model, when such an ingress signal light goes through a beamsplitter, the electric field at the egress sides, can be written as

$$E_s(x, y, z, \tau) = E_0 \begin{array}{l} \{tu(y, z)e^{i(k_s x - \omega_s \tau)} \\ \quad + ru(z, x)e^{i[k_s(y+2d) - \omega_s \tau]}\} \end{array} \tag{3}$$

where t and r are respectively the optical transmitance and reflectance of the beamsplitter.

We use s and i to label the variables of the two ingress lights because our example – the HOM experiment – used the signal and idler lights from a parametric down converter. However, through out this article, we make no assumption whether the two ingress lights are generated by a parametric down converter. We do assume their phases are related and their amplitudes are the same. Assuming equal amplitudes is for simplicity of argument and is ignored when introducing the quantum model. However, the phases are correlated is essential.

As with the signal light, we can write the idler light wave function as

$$E_i(x, y, z, \tau) = E_0 \begin{array}{l} \{tu(z, x)e^{i(k_i y - \omega_i \tau)} \\ \quad - r^* u(x, y)e^{i[k_i(x-2d) - \omega_i \tau]}\} \end{array} \tag{4}$$

We need to stress that the E_s expressed above (and similarly E_i) is an eigen solution or a mode of the wave function. Such a mode is different from the free space (or single fiber) mode because the beamsplitter introduces a boundary condition different from the free space. It takes only one path on the ingress side of the beamsplitter but takes both of the egress paths. We call it the ingress-centric mode representation because the mode is confined to only one ingress path. An alternative is what we call the egress-centric mode representation, which is easier for discussing what the detectors observe. With such representation, a mode propagates along one egress path but along both ingress paths. For example, in egress path 1, the mode function is $u(z, x)e^{i(k_1 y - \omega_1 \tau)}$ (ignoring a normalization factor) on the egress side. And the electric field is

$$E_1(x, y, z, \tau) = E_0 u(z, x) e^{i(k_1 y - \omega_1 \tau)}[t + re^{i(2k_1 d)}]. \tag{5}$$

And on the ingress paths,

$$E_1(x,y,z,\tau) = E_0[u(y,z)e^{i(k_1 x-\omega_1\tau)}+u(z,x)e^{i(k_1 y-\omega_1\tau)}]. \tag{6}$$

Apparently, we are assuming $k_1 = k_s = k_i$ above. We can similarly write E_2. In such representation, E_1 and E_2 are what detectors 1 and 2 observe, respectively. If we generalize our discussion to a generic linear optical device or even a circuit of devices, we can write the electric field in terms of its ingress-centric modes $\{v_n\}$ where $n = 1, 2, \cdots, N$ and egress-centric modes $\{v'_m\}$ where $m = 1, 2, \cdots, M$,

$$\begin{aligned} E(x,y,z,\tau) &= \sum_n^N \mathbb{E}_n v_n(x,y,z)e^{-i\omega_n\tau} \\ &= \sum_m^M \mathbb{E}'_m v'_m(x,y,z)e^{-i\omega_n\tau}. \end{aligned} \tag{7}$$

We can write

$$\mathbb{E}'_m = \sum_n^N \alpha_{m,n}\mathbb{E}_n \tag{8}$$

with

$$\alpha_{m,n} = \int \mathrm{d}x\mathrm{d}y\mathrm{d}z v'^*_m(x,y,z)v_n(x,y,z)\delta_{\omega_m,\omega_n}. \tag{9}$$

Here we assume the modes are orthonormal to each other within their own set. And $\delta_{\omega_m,\omega_n}$ is the Kronecker delta function, which is one when $\omega_m = \omega_n$ and is zero otherwise. Further the matrix $[\alpha_{m,n}]$ is unitary if and only if the modes are orthonormal within their own set. We will find the importance of the matrix $[\alpha_{m,n}]$ in the section on quantum model.

We now come back to the beamsplitter in HOM experiment. If we assume the transmitance t is a real number, ignoring any absolute phase shift, and the reflectance r introduces a relative phase shift of θ, or $r = |r|e^{i\theta}$, we see that the reflected idler wave experiences a phase shift different from that of the signal except when the $\theta + 2kd$ is 90 or 270 degrees. That means, under these exceptional phase shift conditions, the peaks and valleys of the transmitted signal and idler lights are completely offset from those of reflected lights, and therefore the probably of detecting them simultaneously is zero. This is a result of classical wave interference. We shall see more clearly from both the classical and quantum models below that this is one of the factors leading to the HOM effect. A symmetric beamsplitter has θ being 90 or 270 degrees and conveniently put the HOM effect dip at $d = 0$. However, the convenience is only for theoretic derivation and does not affect experiments one way or another.

The HOM experiment uses pulsed lights, which are assembles of spectrum of frequencies. Instead of writing the frequency distributions, we assume the equivalent wavevector distributions are $\phi(k)$ – the same for k_s and k_i. If we assume the Fourier transform of $\phi(k)$ is $\Phi(x)$, we have

$$\begin{aligned} E_1(x,y,z,\tau) = E_0 u(z,x)\ \ &[t\Phi(y-c\tau) \\ &+r\Phi(y+2d-c\tau)] \end{aligned} \tag{10}$$

and

$$\begin{aligned} E_2(x,y,z,\tau) = E_0 u(y,z)\ \ &[t\Phi(x-c\tau) \\ &-r^*\Phi(x-2d-c\tau)] \end{aligned} \tag{11}$$

B. Detection and correlation probability

The detectors count the number of electrical pulses they register. In the classical model, the counting rate are proportional to the intensities of the electrical fields, and the coincident probability of detecting at both detectors within the counting period is proportional to the product of detecting in both detectors.

The HOM experiment has counting periods much longer than the optical pulses. However, it is beneficial if we look into a different scenario in which the counting period is shorter than the optical pulses. Conducting an experiment of such scenario shall offer an alternative to verify our model and interpretation of the HOM effect. Further, the result which we derive for this scenario offers much better understanding of the interference factors, which may contribute to HOM effect. In such an experiment, the coincident probability is

$$\begin{aligned} P_{1,1}(\tau) &\propto |E_1(0,D,0,\tau)|^2|E_2(D,0,0,\tau)|^2 \\ &\propto |\,|t|^2\Phi(D-c\tau)\Phi(D-c\tau) \\ &\quad -|r|^2\Phi(D+2d-c\tau)\Phi(D-2d-c\tau) \\ &\quad +tr\Phi(D+2d-c\tau)\Phi(D-c\tau) \\ &\quad -tr^*\Phi(D-c\tau)\Phi(D-2d-c\tau)\,|^2 \end{aligned} \tag{12}$$

We see that the above is a result of 4 terms with clear origins:

- The $|t|^2$ term: Detector 1 detects the transmitted idler light through the beamsplitter, and detector 2 detects the transmitted signal
- The $|r|^2$ term: Detector 1 detects the reflected signal light, and detector 2 detects the reflected idler
- The tr term: Detector 1 and 2 detect respectively the reflected and transmitted signal light
- The tr^* term: Detector 1 and 2 detect respectively transmitted and reflected idler.

We see that the first and second terms are due to signal and idler lights interfering with each other. Their sum is zero for a symmetric 50/50 beamsplitter when $d = 0$, and the width of the dip around $d = 0$ depends on the pulse width. The cancellation of these two terms is due to phase shift difference of the reflected signal and idler lights by the beamsplitter as we discussed above. The third and fourth terms, however, are due to respectively signal interfering with itself and idler with itself. They oscillate in the scale of the optical wavelength, and thus their sum is not zero. However we can predict, even before we go into the quantum model, that both the third and fourth terms should vanish in the quantum extreme

of single signal or idler photon, in which there is no second photon for self-interference. We will see that vanishing of these terms is the reason behind HOM effect.

We now come to the HOM experiment, which has photon counting periods much longer than the widths of pulses but shorter than the interval between two consecutive pulses. The probability of detecting in each detector is proportional to the total energy received, which is the field intensity integrated over the period, which can be considered infinite for the integration:

$$\begin{aligned} P_{1,1} &\propto [1 + trg(2d) + tr^* g(-2d)] \\ &\quad [1 - trg(2d) - tr^* g(-2d)] \\ &\propto 1 - [trg(2d) + tr^* g(-2d)]^2 \end{aligned} \tag{13}$$

where

$$g(x) = \frac{1 + \int_{-\infty}^{\infty} ds \;\; \Phi(s+x)\Phi^*(s)}{\int_{-\infty}^{\infty} ds \;\; \Phi(s)\Phi^*(s)}. \tag{14}$$

Obviously, the tr and tr^* terms in 13 are from signal and idler interference in detector 1 and 2 respectively. However, the first term "1" includes both 1) signal and idler self interferences, which are correlated, and 2) light pulses, which are not correlated but fall into the same counting period. Technically, $P_{1,1}$ measured this way loses the true meaning of correlation.

In the HOM experiment, the spectrum distribution is assumed Gaussian shaped with wavevector half width (stanard deviation) of K. We have

$$P_{1,1} \propto 1 - 2|tr|^2 e^{-2(Kd)^2} \tag{15}$$

which is the classical result.

III. QUANTUM MODEL

A. Operators and modes

We now turn to describe the quantum model of photons going through a generic linear optical device or a circuit of devices as done for beamsplitters by Fearn and Loudon[8]. In the quantum picture, the electrical fields themselves are quantum operators. We can following the treatment of any quantum optics textbook such as the one by Schubert[17] to rewrite an electrical field operator into portions representing the wave and particle separately. First, we write the electrical field operator as the sum of the positive and negative frequency operators, we get

$$\hat{E}(x,y,z,\tau) = \hat{E}^+(x,y,z,\tau) + \hat{E}^-(x,y,z,\tau). \tag{16}$$

And then we write the positive and negative frequency operators in terms of the mode functions $v_n(x,y,z)e^{i\omega_n \tau}$ and $v_n(x,y,z)e^{-i\omega_n \tau}$ respectively along with the corresponding creation and annihilation operators $\hat{a}_n^\ddagger$ and $\hat{a}_n$ of all the modes $n = 1, 2, 3, \cdots$. For example,

$$\hat{E}^-(x,y,z,\tau) = \sum_n \mathbb{E} v_n(x,y,z) e^{-i\omega_n \tau} \hat{a}_n \tag{17}$$

Here $\mathbb{E}$ is a unit conversion and normalization factor. Clearly, the wave nature is represented in the the mode functions, and the particle nature in the creation and annihilation operators.

As we have shown in the classifcal wave model, there can be several sets of modes. If $\{v_n\}$ and $\hat{a}_n$ above are for the ingress side and $\{v'_m\}$ and $\hat{a'}_m\}$ are for the egress side, the operator equivalent of Eq. 7, 8 and 9 give us

$$\hat{a}'_m = \sum_n \alpha_{m,n} \hat{a}_n. \tag{18}$$

We now have that the quantum operators of the egress and ingress ports related by the $[\alpha_{m,n}]$ matrix given in the classical wave model. Similarly, we can write $\hat{a}_n = \sum_m \alpha'_{n,m} \hat{a}'_m$ and derive $\alpha'_{n,m}$ with the orthonormal assumption. For the simple case of a beamsplitter with $\omega_s = \omega_i$, the annihilation operators in the egress-centric modes is the simplest when we try to calculate the outcome of the photon detectors:

$$\hat{a}'_1 = r\hat{a}_1 + t\hat{a}_2, \quad \text{and} \quad \hat{a}'_2 = t\hat{a}_1 - r^*\hat{a}_2. \tag{19}$$

This is a same result given by the other models[1].

We can extend our results to derive the photon state in the egress mode representation in relation to those in the ingress representation. Assume in the ingress representation, the photon state is $|N_1, N_2, \cdots\rangle$, which represents $N_1, N_2, \cdots$ photons in the respective degenerate and orthonormal modes $\{v_1, v_2, \cdots\}$. The modes all have the same angular frequency: $\omega_1 = \omega_2 = \cdot\omega_n = \cdot$. We can write the same quantum state in a different set of degenerate and othonormal modes $\{v'_1, v'_2, \cdots\}$ as

$$\begin{aligned} &|N_1, N_2, \cdots\rangle \\ = &\sum_{\substack{N'_1+N'_2+\cdots \\ =N_1+N_2+\cdots}} b_{N'_1,N'_2,\cdots} |N'_1, N'_2, \cdots\rangle \end{aligned} \tag{20}$$

Here, the principle that the change of mode representation does not change the photons is important, and thus we require $N'_1 + N'_2 + \cdots = N_1 + N_2 + \cdots$. We can derive the coefficients of the new representation if we consider that

$$\begin{aligned} &b_{N'_1,N'_2,\cdots} \\ = &\langle N'_1, N'_2, \cdots | \, N_1, N_2, \cdots\rangle \\ = &\langle 0, 0, \cdots | \, \tfrac{(\hat{a}'_1)^{N'_1}(\hat{a}'_2)^{N'_2\cdots}}{N'_1! N'_2! \cdots} \, |N_1, N_2, \cdots\rangle \end{aligned} \tag{21}$$

And from Eq. (18), we can express $\{\hat{a'}_1, \hat{a'}_2, \cdots\}$ in terms of $\{\hat{a}_1, \hat{a}_2, \cdots\}$ and thus write $b_{N'_1,N'_2,\cdots}$ in terms of the elements of matrix $[\alpha_{m,n}]$. For the simplest case of a beamsplitter with photons $N_1 = N_2 = 1$ in the ingress mode representation and $\omega_s = \omega_i$ and $d = 0$, we can derive the $b_{N'_1,N'_2}$s and write the photon state in the egress mode representation as

$$tr\,|2,0\rangle - tr^*\,|0,2\rangle + (\,|\,t\,|^2 - |\,r\,|^2)\,|1,1\rangle \tag{22}$$

This is the same result as given in paper by Hong et al[9]. For a 50/50 beamsplitter, the probability of the photons

in the $|1,1\rangle$ state in the egress-mode representation is zero. However, this is due to the phase relation of the modes and is not due to any quantum interference. In fact, for any $N_1 = N_2 = N$, the the probability of the photons in the $|N,N\rangle$ state in the egress-mode representation is zero while that of the $|N-i, N+i\rangle$ states in the egress-mode representation are not zero. Here $i = 1, \cdots N-1$.

B. Photon counting and correlation probability

We now describe the quantum model of photon detection. Let's assume the combined initial quantum state of the signal and idler photons and the electrons in the detectors before the photon-electron interaction at time τ_0 is $|N_s, N_i; 0, 0\rangle$, which consists of N_s signal and N_i idler photons and zero excited state electrons in detector 1 and 2. We assume that there are large pools of electrons in the lower band states, and all the excited/upper band states are vacant so that we can ignore most of the details of the electrons including the exclusive nature as fermions. Let's assume the electrons in the detectors start to interact with the photons at time $\tau = \tau_0$. The photon-electron interaction is described by a dipole interaction Hamiltonian, $H_{int} = -\hat{d}\hat{E}$[17]. We can write the resulting combined quantum state as a superposition of the eigenstates of the un-perturbed combined Hamiltonian H_0:

$$\begin{aligned} & |\Psi(\tau)\rangle \\ = & \sum_{\substack{N_s'+N_i'+n_1'+n_2' \\ =N_s+N_i}} b_{N_s',N_i';n_1',n_2'}(\tau,k_s,k_i)\,|N_s',N_i';n_1',n_2'\rangle \end{aligned} \tag{23}$$

Here we assume the single frequency case and $k_s = k_i$. From Schroedinger equation,

$$\frac{\partial\,|\Psi(\tau)\rangle}{\partial\tau} = (H_0 + H_{int})\,|\Psi(\tau)\rangle \tag{24}$$

we have

$$\begin{aligned} & \tfrac{d}{d\tau} b_{N_s',N_i';n_1',n_2'}(\tau,k_s,k_i) \\ = & \sum_{N"_s+N_i''+n"_1+n"_2=N_s+N_i} \\ & \left\langle N"_s, N"_i; n"_1, n"_2\,|H_{int}|\,N_s^{'}, N_i^{'}; n_1^{'}, n_2^{'}\right\rangle \end{aligned} \tag{25}$$

Approximate to the first order, we can derive the coefficients $b_{N"_s,N"_i;n"_1,n"_2}(\tau,k_s,k_i)$. For example,

$$\begin{aligned} & b_{N_s-1,N_i;1,0}(\tau,k_s,k_i) \\ = & \int_{\tau_0}^{\tau} d\tau_1 \int dxdydz\,\langle N_s-1,N_i;1,0\,|H_{int}|\,N_s,N_i;0,0\rangle \end{aligned} \tag{26}$$

and

$$\begin{aligned} & b_{N_s-2,N_i;1,1}(\tau,k_s,k_i) \\ = & \int_{\tau_0}^{\tau} d\tau_1 b_{N_s-1,N_i;1,0}(\tau_1,k_s,k_i)\int dxdydz \\ & \langle N_s-2,N_i;1,1\,|H_{int}|\,N_s-1,N_i;1,0\rangle \\ + & \int_{\tau_0}^{\tau} d\tau_1\, b_{N_s-1,N_i;0,1}(\tau_1,k_s,k_i)\int dxdydz \\ & \langle N_s-2,N_i;1,1\,|H_{int}|\,N_s-1,N_i;0,1\rangle \\ = & b_{N_s-1,N_i;1,0}(\tau,k_s,k_i)\,b_{N_s-2/N_s-1,N_i;0,1}(\tau,k_s,k_i) \end{aligned} \tag{27}$$

Here

$$\begin{aligned} & b_{N_s-2/N_s-1,N_i;0,1}(\tau,k_s,k_i) \\ = & \int_{\tau_0}^{\tau} d\tau_1 \int dxdydz \\ & \langle N_s-2,N_i;1,1\,|H_{int}|\,N_s-1,N_i;0,1\rangle \end{aligned} \tag{28}$$

represents that a photon is absorbed by an electron in the transition from the $|N_s-1,N_i;0,0\rangle$ state to the $|N_s-2,N_i;0,1\rangle$ state. Similarly, we have

$$\begin{aligned} & b_{N_s,N_i-2;1,1}(\tau,k_s,k_i) \\ = & b_{N_s,N_i-1;1,0}(\tau,k_s,k_i)\,b_{N_s,N_i-2/N_i-1;0,1}(\tau,k_s,k_i) \end{aligned} \tag{29}$$

and

$$\begin{aligned} & b_{N_s-1,N_i-1;1,1}(\tau,k_s,k_i) \\ = & b_{N_s,N_i-1;0,1}(\tau,k_s,k_i)\,b_{N_s-1,N_i;1,0}(\tau,k_s,k_i) \\ + & b_{N_s,N_i-1;1,0}(\tau,k_s,k_i)\,b_{N_s-1,N_i;0,1}(\tau,k_s,k_i) \end{aligned} \tag{30}$$

Detecting photons in detector 1 or 2 is to look up whether electrons are in the upper band excited states:

$$\sum_{n_1,n_2} B_{n_1,n_2}(\tau,k_s,k_i)\,|n_1,n_2\rangle \tag{31}$$

with $n_1 > 0$ and/or $n_2 > 0$. The photon detection results depend on summing up all the photon states and looking at only the electron states:

$$\begin{aligned} & B_{1,0}(\tau,k_s,k_i) \\ = & b_{N_s-1,N_i;1,0}(\tau,k_s,k_i) + b_{N_s,N_i-1;1,0}(\tau,k_s,k_i) \end{aligned} \tag{32}$$

$$\begin{aligned} & B_{0,1}(\tau,k_s,k_i) \\ = & b_{N_s-1,N_i;0,1}(\tau,k_s,k_i) + b_{N_s,N_i-1;0,1}(\tau,k_s,k_i) \end{aligned} \tag{33}$$

and

$$\begin{aligned} & B_{1,1}(\tau,k_s,k_i) \\ = & b_{N_s-2,N_i;1,1}(\tau,k_s,k_i) + b_{N_s,N_i-2;1,1}(\tau,k_s,k_i) \\ + & b_{N_s-1,N_i-1;1,1}(\tau,k_s,k_i) \\ = & b_{N_s-1,N_i;1,0}(\tau,k_s,k_i)\,b_{N_s-2/N_s-1,N_i;0,1}(\tau,k_s,k_i) \\ + & b_{N_s,N_i-1;1,0}(\tau,k_s,k_i) b_{N_s,N_i-2/N_i-1;0,1}(\tau,k_s,k_i) \\ + & b_{N_s-1,N_i;1,0}(\tau,k_s,k_i) b_{N_s,N_i-1;0,1}(\tau,k_s,k_i) \\ + & b_{N_s-1,N_i;0,1}(\tau,k_s,k_i) b_{N_s,N_i-1;1,0}(\tau,k_s,k_i) \end{aligned} \tag{34}$$

When N_s and N_i are large, we can imagine that the terms involving N_s-2 and N_i-2 are the same as those of N_s-1 and N_i-1, and $B_{1,1}(\tau,k_s,k_i) =$

$B_{1,0}(\tau,k_s,k_i)B_0,1(\tau,k_s,k_i)$ and that the photon detection results shall be no different from the classical results. In the quantum extreme of single photons, $N_s=N_i=1$, the N_s-2 and N_i-2 terms will vanish.

We now shall look into photon detection with the following assumptions to simplify the calculation:

- For photon detection, we only need to consider the photon annihilation portion of the interaction Hamiltonian, which is $H_{int}=-\hat{d}^+\hat{E}^-$;
- The detectors have wide and flat spectral responses that the electron dipole moment in each detector is the same across the entire spectrum in concern;
- The optical wavelengths are much longer than that of an electron, and the mode functions can be assumed constant within the space where an electron interacts with a photon. Therefore, the spatial integrations only involve electron dipole moments;
- The photon-electron interaction process is of much shorter time than the photon counting period or the optical wave pulses.

If we write at detector 1,

$$\begin{aligned}&\hat{E}^-(0,D_1,0,\tau)\\ =\;& r\hat{E}_s^-(0,D,0,\tau)+tE_i^-(0,D,0,\tau)\\ =\;& r\mathbb{E}u(0,0)e^{i(k_sD+2k_sd-\omega_s\tau)}\hat{a}_s\\ +\;& t\mathbb{E}u(0,0)e^{i(k_iD-\omega_i\tau)}\hat{a}_i\end{aligned}\tag{35}$$

and at detector 2,

$$\begin{aligned}&\hat{E}^-(D_2,0,0,\tau)\\ =\;& t\mathbb{E}u(0,0)e^{i(k_sD-\omega\tau)}\hat{a}_s\\ -\;& r^*\mathbb{E}u(0,0)e^{(i(k_iD-2k_id-\omega\tau)}\hat{a}_i\end{aligned}\tag{36}$$

we can write

$$\begin{aligned}&b_{N_s-1,N_i;1,0}(\tau,k_s,k_i)\\ =\;& \int_{\tau_0}^{\tau}d\,\tau_1\int_{V_1}dxdydz\\ & r\sqrt{N_s}\mathbb{E}u(0,0)e^{i(k_sD+2k_sd-\omega_s\tau)}\langle 1,0\left|-\hat{d}^+\right|0,0\rangle\\ =\;& rt\sqrt{N_s}\int_{\tau_0}^{\tau}d\tau_1e^{i(k_sD+2k_sd-\omega_s\tau)}M_1\end{aligned}\tag{37}$$

where V_1 is the volume of detector 1 and M_1 reflects the electron dipole moment:

$$M_1=\mathbb{E}u(0,0)\int_{V_1}dxdydz\langle 1,0\left|-\hat{d}^+\right|0,0\rangle\tag{38}$$

We can also write

$$b_{N_s,N_i-1;1,0}(\tau,k_s,k_i)=t\sqrt{N_i}\int_{\tau_0}^{\tau}d\tau_1e^{i(k_iD-\omega_i\tau)}M_1\tag{39}$$

$$b_{N_s-1,N_i;0,1}(\tau,k_s,k_i)=t\sqrt{N_s}\int_{\tau_0}^{\tau}d\tau_1e^{i(k_sD-\omega_s\tau)}M_2\tag{40}$$

$$\begin{aligned}&b_{N_s,N_i-1;0,1}(\tau,k_s,k_i)\\ =\;& -r^*\sqrt{N_i}\int_{\tau_0}^{\tau}d\tau_1e^{i(k_iD-2k_id-\omega_i\tau)}M_2\end{aligned}\tag{41}$$

If we take into consideration that the signal and idler lights are assembles of spectrum of wavevectors, we have

$$\begin{aligned}&B_{1,1}(\tau)\\ =\;& \int_{-\infty}^{\infty}dk_s\phi(k_s)\int_{-\infty}^{\infty}dk_i\phi(k_i)\\ [\;& b_{N_s-1,N_i;1,0}(\tau,k_s,k_i)b_{N_s-2/N_s-1,N_i;0,1}(\tau,k_s,k_i)\\ +\;& b_{N_s,N_i-1;1,0}(\tau,k_s,k_i)b_{N_s,N_i-2/N_i-1;0,1}(\tau,k_s,k_i)\\ +\;& b_{N_s-1,N_i;1,0}(\tau,k_s,k_i)b_{N_s,N_i-1;0,1}(\tau,k_s,k_i)\\ +\;& b_{N_s-1,N_i;0,1}(\tau,k_s,k_i)b_{N_s,N_i-1;1,0}(\tau,k_s,k_i)]\end{aligned}\tag{42}$$

In the scenario that photon counting period is shorter than the optical pulses, we have

$$\begin{aligned}&P_{1,1}(\tau)=|B_1,1(\tau)|^2\\ \propto\;& |\,|t|^2\sqrt{N_sN_i}\Phi_s(D-c\tau)\Phi_i(D-c\tau)\\ -\;& |r|^2\sqrt{N_sN_i}\Phi_i(D-2d-c\tau)\Phi_s(D+2d-c\tau)\\ +\;& tr\sqrt{(N_s-1)N_s}\Phi_s(D-c\tau)\Phi_s(D+2d-c\tau)\\ -\;& tr^*\sqrt{(N_i-1)N_i}\Phi_i(D-2d-c\tau)\Phi_i(D-c\tau)\,|^2\end{aligned}\tag{43}$$

All the terms have their corresponding ones in the classical wave model. Obviously, when $N_s=N_i=1$, the self-interference terms vanish. And in the case $\Phi(x)$ being a Gaussian shaped pulse,

$$P_{1,1}(\tau)=|B_{1,1}(\tau)|^2\propto|t^2-r^2e^{-(2Kd)^2}|^2e^{-K^2(D-c\tau)^2}\tag{44}$$

We see that $P_{1,1}(\tau)$ is also reverse bell shaped but with a different width from the HOM experiment – $1/(2\sqrt{2}K)$ vs. $1/(\sqrt{2}K)$. An experiment may be designed to verify this difference and thus validate the model. Such an experiment is more difficult than the HOM experiment because the detection period is only a portion of a photon pulse width – the opposite to the HOM experiment. This difficulty may be compensated by repeating the counting many many times, a technique also used in the HOM experiment.

In the HOM experiment, the photon counting period is much longer than the optical pulses and can be considered infinite, the coincident probability is

$$\begin{aligned}&P_{1,1}\\ =\;& \int_{(-\infty)}^{(\infty)}d\tau_1\int_{(-\infty)}^{(\infty)}d\tau_2|M_1M_2|^2\\ [\;& tr\sqrt{(N_s-1)N_s}\Phi_s(D-c\tau_1)\Phi_s(D+2d-c\tau_2)e^{2ik_0d}\\ -\;& tr^*\sqrt{(N_i-1)N_i}\Phi_i(D-2d-c\tau_1)\Phi(D-c\tau_2)e^{-2ik_0d}\\ -\;& |r|^2\sqrt{N_sN_i}\Phi_i(D-2d-c\tau_1)\Phi_s(D+2d-c\tau_2)\\ +\;& t^2\sqrt{N_sN_i}\Phi_i(D-c\tau_1)\Phi_s(D-c\tau_2)]^2.\end{aligned}\tag{45}$$

When $N_s = N_i = 1$, the signal or idler self-interference terms vanish, and

$$P_{1,1} \propto |t|^4 + |r|^4 - 2|tr|^2|g(2d)|^2 \tag{46}$$

It is the same result as given in the HOM paper. Clearly, variation of $P_{1,1}$ by d depends on $\phi(k)$. If $\phi(k)$ is of Gaussian distribution, the optical pulse shape $\Phi(x)$ and $|g(2d)|^2$ are all of Gaussian shape, and $P_{1,1}$ is of upside-down bell shape. The reason that some other similar experiments[18] that see $P_{1,1} - d$ variation different from the upside-down bell shape is because their $\phi(k)$ are different from Gaussian distribution.

IV. CONCLUSION

We have shown that a quantum optic model can be developed to describe photons traversing linear optical devices from the first quantum principle without additional assumptions or restrictions. It is generic and powerful – it can be applied to modeling a circuit of linear optical devices of arbitrary ingress and egress ports. We have applied the model to explain the HOM effect without introducing any quantum interference. HOM effect is due to lack of signal-signal or idler-idler self-interference in the quantum extreme of single signal and idler photons and leaving signal-idle interference dominant.

[1] E. Knill, R. Laflamme, and G. J. Milburn. A scheme for efficient quantum computation with linear optics. *Nature*, 409(6816):46–52, Jan 2001.

[2] Jianwei Wang, Stefano Paesani, Yunhong Ding, Raffaele Santagati, Paul Skrzypczyk, Alexia Salavrakos, Jordi Tura, Remigiusz Augusiak, Laura Mančinska, Davide Bacco, Damien Bonneau, Joshua W. Silverstone, Qihuang Gong, Antonio Acín, Karsten Rottwitt, Leif K. Oxenløwe, Jeremy L. O'Brien, Anthony Laing, and Mark G. Thompson. Multidimensional quantum entanglement with large-scale integrated optics. *Science*, 360(6386):285–291, 2018.

[3] Pieter Kok, W. J. Munro, Kae Nemoto, T. C. Ralph, Jonathan P. Dowling, and G. J. Milburn. Linear optical quantum computing with photonic qubits. *Rev. Mod. Phys.*, 79:135–174, Jan 2007.

[4] Nicolas C. Menicucci. Temporal-mode continuous-variable cluster states using linear optics. *Phys. Rev. A*, 83:062314, Jun 2011.

[5] François Hénault. Quantum physics and the beam splitter mystery. In Chandrasekhar Roychoudhuri, Al F. Kracklauer, and Hans De Raedt, editors, *The Nature of Light: What are Photons? VI*, volume 9570, pages 199 – 213. International Society for Optics and Photonics, SPIE, 2015.

[6] Richard A. Campos, Bahaa E. A. Saleh, and Malvin C. Teich. Quantum-mechanical lossless beam splitter: Su(2) symmetry and photon statistics. *Phys. Rev. A*, 40:1371–1384, Aug 1989.

[7] Richard A. Campos, Bahaa E. A. Saleh, and Malvin C. Teich. Fourth-order interference of joint single-photon wave packets in lossless optical systems. *Phys. Rev. A*, 42:4127–4137, Oct 1990.

[8] H. Fearn and R. Loudon. Quantum theory of the lossless beam splitter. *Optics Communications*, 64(6):485 – 490, 1987.

[9] Chua Hong, ZY Ou, and L Mandel. Measurement of subpicosecond time intervals between two photons by interference. *Physical review letters*, 59:2044–2046, 12 1987.

[10] Vittorio Degiorgio. Phase shift between the transmitted and the reflected optical fields of a semireflecting lossless mirror is $\pi/2$. *American Journal of Physics*, 48(1):81–81, January 1980.

[11] J. L. O'Brien, G. J. Pryde, A. G. White, T. C. Ralph, and D. Branning. Demonstration of an all-optical quantum controlled-not gate. *Nature*, 426(6964):264–267, Nov 2003.

[12] Adrian J. Menssen, Alex E. Jones, Benjamin J. Metcalf, Malte C. Tichy, Stefanie Barz, W. Steven Kolthammer, and Ian A. Walmsley. Distinguishability and many-particle interference. *Phys. Rev. Lett.*, 118:153603, Apr 2017.

[13] T. B. Pittman, D. V. Strekalov, A. Migdall, M. H. Rubin, A. V. Sergienko, and Y. H. Shih. Can two-photon interference be considered the interference of two photons? *Phys. Rev. Lett.*, 77:1917–1920, Sep 1996.

[14] J. Beugnon, M. P. A. Jones, J. Dingjan, B. Darquié, G. Messin, A. Browaeys, and P. Grangier. Quantum interference between two single photons emitted by independently trapped atoms. *Nature*, 440(7085):779–782, Apr 2006.

[15] Charles Santori, David Fattal, Jelena Vučković, Glenn S. Solomon, and Yoshihisa Yamamoto. Indistinguishable photons from a single-photon device. *Nature*, 419(6907):594–597, Oct 2002.

[16] Megan R. Ray and S. J. van Enk. Verifying entanglement in the hong-ou-mandel dip. *Phys. Rev. A*, 83:042318, Apr 2011.

[17] M. Schubert and B. Wilhelmi. *Nonlinear optics and quantum electronics*. John Wiley and Sons, 1986.

[18] R. Ghosh and L. Mandel. Observation of nonclassical effects in the interference of two photons. *Phys. Rev. Lett.*, 59:1903–1905, Oct 1987.